International Journal of Mining Science and Technology 26 (2016) 1043–1049

Contents lists available at ScienceDirect

International Journal of Mining Science and Technology

journal homepage: www.elsevier.com/locate/ijmst

Effects of mechanical activation on the structural changes and microstructural characteristics of the components of ferruginous quartzite beneficiation tailings

Ermolovich E.A. [a,*], Ermolovich O.V. [b]

[a] Faculty of Mining and Natural Resource Management, Belgorod State National Research University, Belgorod 308015, Russia
[b] GeoStroyMonitoringBelGU, LTD, Belgorod 308034, Russia

ARTICLE INFO

Article history:
Received 17 July 2015
Received in revised form 9 September 2015
Accepted 23 March 2016
Available online 19 September 2016

Keywords:
Ferruginous quartzite beneficiation tailings
Mechanical activation
Crystallites
Planetary mill
Microstructure
Structural changes

ABSTRACT

The effects of mechanical activation in a planetary mill on the structural changes and microstructural characteristics of the components of ferruginous quartzite beneficiation tailings generated by wet magnetic separation process were studied using X-ray and laser diffraction methods. The results revealed the relationship between variations in the mean particle size of activated powders and the milling time. The crystallite size, microstrain, lattice parameters and unit cell volumes were determined for different milling times in powder samples of quartz, hematite, dolomite, and magnetite from the beneficiation tailings. The main trends in the variation of the crystallite size of quartz, hematite, dolomite, and magnetite as a function mean particle size of powder samples were revealed. Changes in the particle shape as a function of the activation time was also investigated.

1. Introduction

At present, more than one-half of commercial iron ore production in Russia comes from the Kursk Magnetic Anomaly (KMA) basin. Similarly, this region accounts for more than one-half of the tailings from ore beneficiation. Estimates indicate that the amount of iron ore tailings generated and stockpiled on site (together with the existing tailings) within the KMA using the common beneficiation methods may reach 21–24 billion tons over the next fifty years. Tailings from beneficiation process containing up to 80–95% free silica pose potential risk of silicosis. Long-term storage of tailings is usually the biggest environmental concern. Effective utilization of massive tailings resources can require modification of the structure and properties of waste materials.

Mechanical activation or activation grinding is one of the most effective means to cause changes in the structural characteristics and properties of the material during higher-energy milling under the action of mechanical forces compared to the traditional ball millings. Such grinding results in the structural-chemical transformations of minerals, formation of lattice distortion and dislocations and point defects.

The waste materials generated during beneficiation of ferruginous quartzite using the wet magnetic separation process are complex multicomponent mixtures the microstructural changes of which during comminution have yet to be studied.

The goal of this study is to investigate structural and microstructural changes of waste materials induced by mechanical activation, which can be used to develop a novel composite material consisting of dispersed fine particle with substantially enhanced properties. The trends in the change of their microstructure as a function the specific surface area can provide the basis for developing quick test methods for assessment and ranking waste materials in terms of their potential for effective backfill mix design. Void filling using mill tailings especially in metal mining is one of the best techniques [1].

2. Materials and methods

The chemical analysis by X-ray fluorescence on the ARL Optim'X spectrometer revealed that the waste material generated during beneficiation of ferruginous quartzite using the wet magnetic separation process contains (in wt.%) about 59. 82% SiO_2, 20.36% Fe_2O_3, 6.67% CaO, 2.20% MgO, 7.63% CO_2, 1.09% P_2O_5, 0.91% Al_2O_3, 0.438% K_2O, 0.34% Na_2O, 0.274% TiO_2, 0.147% MnO, 0.0705% SO_3, 0.0355% WO_3, 0.0302% SrO, 0.0089% CuO, 0.0026% ZrO_2, and 0.0021%

* Corresponding author. Tel.: +7 920 5546114.
E-mail address: elena.ermolovich@mail.ru (E.A. Ermolovich).

http://dx.doi.org/10.1016/j.ijmst.2016.09.012
2095-2686/

Table 1
Summary of particle size distribution data for powder samples.

Characteristics	Starting size	Milling time 1 h, in ethanol	Milling time 2 h, in ethanol	Milling time 6 h, in ethanol	Milling time 6 h in ethanol +6 h in air	Milling time 12 h, in ethanol
D10[a] (10% of particles) (μm)	11.336	1.020	1.003	0.856	0.727	0.471
D50 (50% of particles) (μm)	59.024	6.035	3.983	2.601	2.071	1.187
D90 (90% of particles) (μm)	141.340	25.770	11.143	7.454	7.252	2.017
Mean particle size, (Mean volume diameter), d[4.3] (μm)	69.16	9.65	5.23	3.46	3.10	1.22
Fraction	Content of fine-grained fractions in the bulk sample (%)					
0–1 μm	1.61	12.27	14.85	17.29	22.76	47.90
0–3 μm	4.30	36.24	40.15	49.98	66.82	99.91
0–5 μm	5.63	45.38	53.14	72.28	74.21	100.00
0–10 μm	9.17	65.66	85.54	97.38	97.36	100.00

Note:
[a] D10 is the particle size at which 10% of the particles are finer; D50 is the grain size at which 50% of the particles are finer; D90 is the particle size at which 90% of the particles are finer.

Y_2O_3. The XRD spectra were recorded using an Ultima IV Rigaku diffractometer (Cu K_α, $\lambda = 0.154059$ nm, in the range of $2\theta = 10$–$110°$ at the step size of $\Delta(2\theta) = 0.02°$ and scanning speed of 2.5 s) and contained the diffraction lines from quartz SiO_2 (ICDD PDF-2# 00-046-1045), hematite Fe_2O_3 (ICDD PDF-2# 01-086-0550), magnetite (ICDD PDF-2# 01-086-1346) Fe_3O_4, and dolomite $CaMg(CO_3)_2$ (ICDD PDF-2# 01-073-2361).

The quantitative analysis of XRD patterns and phase identification were performed using the PDXL RIGAKU software. The diffraction data were smoothed by the Savitsky-Golay method [2] and the background line was subtracted using the Sonneveld-Visser method [3]. The diffractions were described by a Gaussian function and the Rachinger correction was applied to separate a diffraction peak doublet into the $K_{\alpha1}$ and $K_{\alpha2}$ components [4]. The mean crystallite (Coherently Scattering Domains (CSD)) size (D) for quartz, hematite, magnetite, and dolomite was determined from the β line broadening analysis. The instrumental angular resolution function of the diffractometer $\mathrm{FWHM_R} = (utg^2\theta + vtg\theta + w)^{1/2}$, where $u = 0.0093$, $v = -0.0090$ and $w = 0.0078$ was determined in a special diffraction experiment using a standard sample of the lanthanum hexaboride LaB_6 (PRF-12). The X-ray diffraction peak broadening $\beta = (\mathrm{FWHM}^2_{exp} - \mathrm{FWHM}^2_R)^{1/2}$ was determined by comparing the full width at half-maximum of an experimental diffraction reflection FWHM^2_{exp} with the instrumental angular resolution function of the diffractometer FWHM^2_R [5]. The mean crystallite size D and the contribution from the microstrain ε were determined using the Williamson-Hull plot [6] based on an approximation that the functions of size and strain contributions are described by the Gaussian functions [7]:

$$\beta^2 \cdot \cos^2\theta = (4\varepsilon \sin\theta)^2 + \left(\frac{\lambda}{D}\right)^2 \quad (1)$$

where θ is the Bragg angle, β is the broadening of the diffraction line, ε is the microstrain, and λ is the X-ray wavelength.

The plot of $\left(\frac{\beta\cdot\cos\theta}{\lambda}\right)^2$ vs. $\left(\frac{4\sin\theta}{\lambda}\right)^2$ is a straight line with the tangent of the inclination angle proportional to ε^2 and the y-intercept inversely proportional to D^2.

The tailings samples were ground to powder in a Pulverisette 5 laboratory planetary ball mill at 400 r/min with automatic time reverse rotation every 30 min. For each run, maximum powder batches of 210 g were ground using one 250 ml stainless steel jar with balls of 5–20 mm diameter and 790 g total weight. The powders were milled in air and 60 ml ethanol for intervals of 1–12 h and dried after milling.

The particle size distribution and elongation ratio were determined with an Analysette 22 NanoTec Laser Diffraction Analyzer using the wet dispersion and ultrasonication of the sample powder [8]. The Analysette 22 NanoTec is the instruments which produces a particle size distribution and particle shape analysis (elongation ratio) in a single measurement.

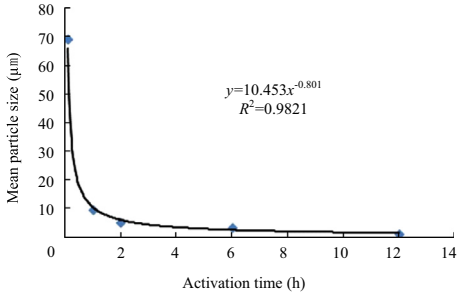

Fig. 1. Variation of the mean particle size as a function of the activation time.

Fraunhofer theory was applied for interpretation of diffraction pattern for determining particle size. The elongation was defined as the ratio of the radii of the ellipsoid.

3. Results and discussion

3.1. Particle size and shape

The tailings samples with an initial mean particle size of 69.16 μm were milled in ethanol at intervals of 1, 2, and 6 h to sequentially reduce the mean particle sizes to 9.65, 5.23 and 3.46 μm, respectively, then the powders were milled for 6 h in ethanol and 6 h in air to particle size of 3.1 μm; and finally the samples were milled in ethanol for 12 h to a mean particle size of 1.22 μm. The data on the particle size distribution in fine-grained fractions are summarized in Table 1. Changes in the mean volume diameter of the particles as a function of the milling time are shown in Fig. 1.

The experimental data indicate that after 2 h of milling over 85% of the material was milled to the particle size below 10 μm. The degree of crystallinity of fine mineral particles below 10 μm is becoming increasingly important because fine milling is capable of producing novel crystalline materials with crystallite sizes at the nanometer scale in which tailored properties can be used to improve hydrometallurgical processes, reduce annealing temperature, accelerate the reactivity of the binders, allow for the formation of metastable phases and particles with high surface energies [9]. Although a substantial difference was found in the particle size after 1, 2, 6, and 12 h of milling, intensive grinding

of high purity hematite in the planetary mill after 3 and 9 h of milling produced no differences in the particle size grain [10]. This effect was probably a result of the formation of agglomerates during extended milling of different minerals [11–14], which appears to have been eliminated in the experiments conducted using wet milling in an aqueous medium and an ultrasonic bath.

While it is widely recognized that comminution can lead to changes in particle shape, relatively few attempts have been made to quantify the parameters of ground minerals and ores as they relate to comminution processes [10]. To characterize the shape of particles produced by milling of ferruginous quartzite tailings, this study applied one of the main shape descriptors such as elongation, the values of which are shown in Table 2.

The elongation ratio increases with increasing milling time, reaching its maximum after 6 h of milling (mean particle size of 3.46 μm) and continues to decrease, reaching its minimum after 12 h of milling (mean particle size of 1.22 μm). Particle shape of the activated powder samples are shown in Fig. 2.

This implies that the shape of particles is controlled by the milling time, which is in agreement with the observations of Kaya et al. [15] for quartz and coal. However Kaya et al. [15] have reported that grinding in a planetary ball mill produces more rounded particles with increasing milling time without increasing elongation ratio till 6 h of milling time followed by a decrease. Also, the observations of the authors are not in agreement with Kuga et al. [16] who however used a screen mill for comminution.

3.2. Amorphization degree

The increase in the abundance of X-ray amorphous material is manifested by decreases in the integral intensity of diffraction lines. The content of X-ray amorphous phase was determined by equation proposed by Ohlberg and Strickler [17]:

$$A = 100 - X\ (\%) \tag{2}$$

$$X = \frac{U_0}{I_0} \cdot \frac{I_x}{U_x} \cdot 100 \tag{3}$$

Table 2
Elongation ratios of the activated powder particles produced by milling of ferruginous quartzite tailings.

Milling time (h)	Mean particle size (μm)	Elongation ratio
0	69.16	2.000
1	9.65	2.320
2	5.23	2.784
6	3.46	3.467
6 + 6	3.10	2.155
12	1.22	1.441

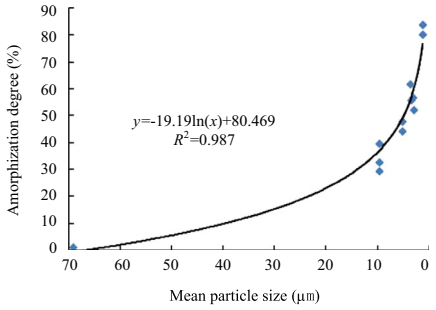

Fig. 3. Degree of amorphization as a function of the mean particle size of quart powders.

where U_0 and U_x refer to the background of non-activated and activated samples while I_0 and I_x are integral intensities of diffraction lines of non-activated and activated samples. A and X denote the degree of amorphization and degree of crystallinity, respectively.

In our calculations, the eight most intensive reflection peaks of quartz, dolomite, and magnetite were used. It is assumed that the amorphous phase in the initial mineral powder is negligible. The portion of X-ray amorphous phase in quartz is shown Fig. 3.

It is clear that the amorphization increases with the increase of the milling time and the decrease of the particle size. The amorphization increases rapidly at the initial stages of milling reaching 25–30% after 1 h of milling (mean particle size of 9.65 μm) and continues to increase to 80% after 12 h of milling when the mean particle size is in the order of 1.22 μm. The increase of X-ray amorphous phase due to intensive milling was reported for quartz, sulfide minerals, calcite, and magnesite [18–22]. Other results were obtained for hematite, magnetite, and dolomite for which the degree of amorphization has not been determined. The calculations show that the degree of crystallinity of all of these minerals increases at all stages of milling. The intensity of the reflection peaks increases considerably up to 6 h of milling and reduces progressively after 12 h of milling, remaining higher than that of the non-activated sample. These results can be explained by the breaking of hematite, magnetite, and dolomite intergrowths in the composition of iron ore tailings. At the same time, the experiments with high-purity hematite [10] showed that after 9 h of milling in the planetary mill, 85% of the initial hematite was converted into amorphous phase. Similar results were obtained after 10 h of milling of hematite powder whose degree of crystallinity ranged from 9.37% to 49.8% [23]. The maximum amorphization degree (80–90%) was achieved for magnetite from the milling in a planetary ball mill after 60 min of grinding [24].

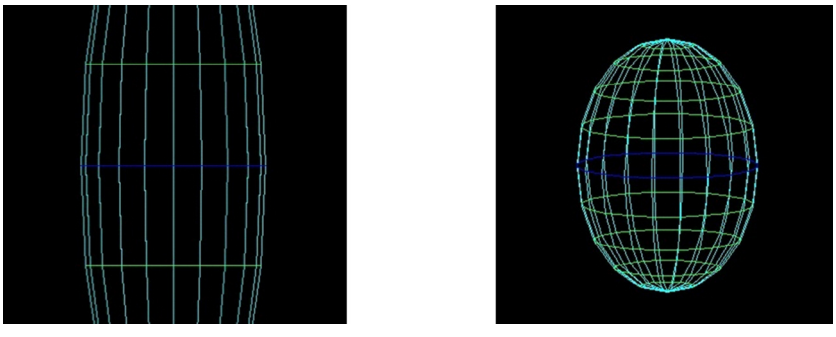

Fig. 2. Particle shape of the activated powder samples after: (a) 6 h of milling time (mean size of 3.46 μm) and (b) 12 h of milling time (mean size of 1.22 μm).

3.3. Microcrystalline characteristics

X-ray diffraction profile analysis is a powerful tool to characterize the microstructure of a material powder obtained during prolonged milling.

The XRD studies do not show phases below 2% by weight. This agrees with the observations of Pourghahramani and Forssberg, Kaczmarek and Ninham, and Stewart et al. [10,25,26].

The diffraction peaks for mechanically activated hematite powder are broader than those for the initial samples. The XRD patterns for powder samples of iron or tailings for different milling times are shown in Fig. 4. (The XRD patterns show shifting of the position of each reflection line to the right during computer processing to prevent the interference and overlapping, which make the observation of structural changes difficult).

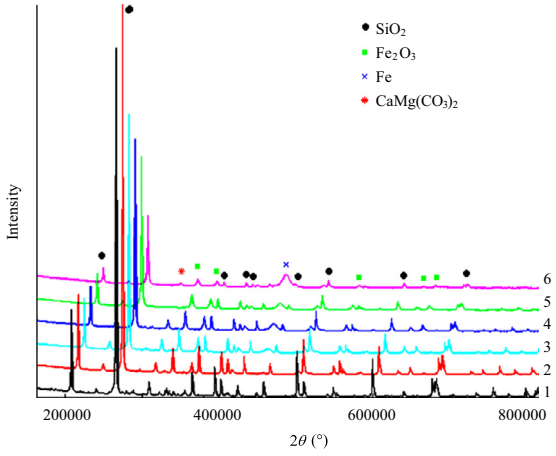

Fig. 4. X-ray diffraction patterns of starting and activated powder samples of ferruginous quartzite tailings generated during wet magnetic separation processes, mean particle size (1–69.16 μm; 2–9.65 μm; 3–5.23 μm; 4–3.46 μm; 5–3.10 μm; 6–1.22 μm).

The XRD patterns for the individual reflections of quartz, hematite, and dolomite are shown in Fig. 5.

Crystallite size is a fundamental property of the material. Changes in the crystallite size during milling were examined in several previous studies [9,12,21].

Our observations indicate a decrease in the average crystallite size (D) of quartz, hematite, magnetite, and dolomite samples depending on the activation time (Table 3).

This is supported by data for hematite. The minimum crystallite size obtained was 17.1 nm when hematite was ground for 10 h [23]. The crystallite size decreased exponentially for quartz, hematite, and dolomite ($D = 137.18e^{-0.151t}$; $D = 86.438e^{-0.118t}$; $D = 14.232e^{-0.058t}$, respectively) and linearly for magnetite ($D = -0.4709t + 10.658$). This is consistent with the experimental results obtained in the previous study [21], which suggested that the decrease in the crystallite size as a function of milling time can be described by different trends for different minerals. The physical broadening of reflection lines due to strain and crystallite size is observed after 12 h of milling (Table 3). For magnetite, the strain contribution to the line broadening is very small and negligible. The variations of crystallite sizes of quartz, hematite, magnetite, and dolomite from the milled samples of iron ore tailings as a function of the mean particle size are shown in Fig. 6. The experimental data are well approximated by a logarithmic function.

In this study, the unit cell parameters for quartz, hematite, magnetite and dolomite from the beneficiation tailings were analyzed as a function of the mechanical activation time (Table 4).

The unit cell parameters were calculated using a least squares method. The unit cell volume of the studied hexagonal systems (quartz, hematite, and dolomite) was calculated by the formula $V = 0.866025a^2c$, where a and c are the unit cell parameters. The cell volume of hematite was defined as $V = a^3$. It was found that all milled samples of quartz, hematite, and dolomite exhibited an expansion of a unit cell and an increase in the lattice parameters as compared to the non-activated powder. The dolomite sample

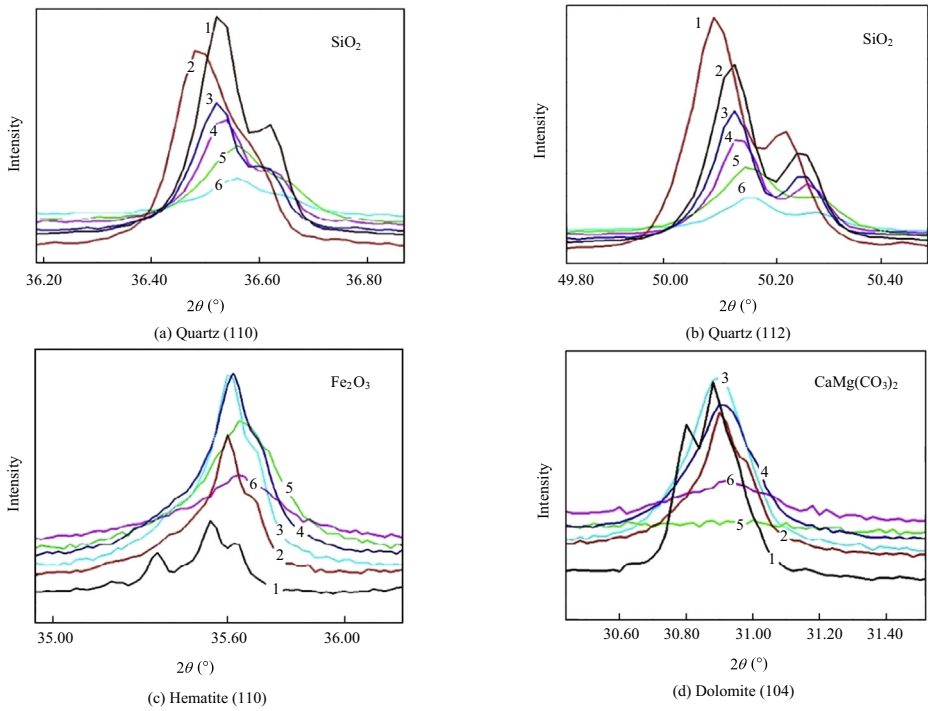

Fig. 5. X-ray diffraction pattern for: (a) quartz (110); (b) quartz (112); (c) hematite (110); and (d) dolomite (104) powder from ferruginous quartzite tailings generated during wet magnetic separation processes, mean particle size (1–69.16 μm; 2–9.65 μm; 3–5.23 μm; 4–3.46 μm; 5–3.1 μm; 6–1.22 μm).

Table 3
Mean crystallite size and lattice strain components obtained for milled samples of iron ore tailings.

Activation time (h) (ethanol)	Mean size of coherently scattering domain, D (nm)				Microstrain, ε (%)		
	Quartz SiO_2	Hematite Fe_2O_3	Magnetite Fe_3O_4	Dolomite $CaMg(CO_3)_2$	Quartz SiO_2	Hematite Fe_2O_3	Dolomite $CaMg(CO_3)_2$
0	149.7	108.6	11.0	14.9	0	0	0
1	110.8	66.9	10.5	12.6	0	0	0
2	86.7	58.2	8.5	12.0	0	0	0
6	67.8	45.3	8.6	11.3	0	0	0
6 h in air + 6 h in ethanol	46.9	24.9	8.8	10.9	0.03	0.11	0.0100
12	20.9	21.1	4.8	6.8	0.03	0.37	0.0108

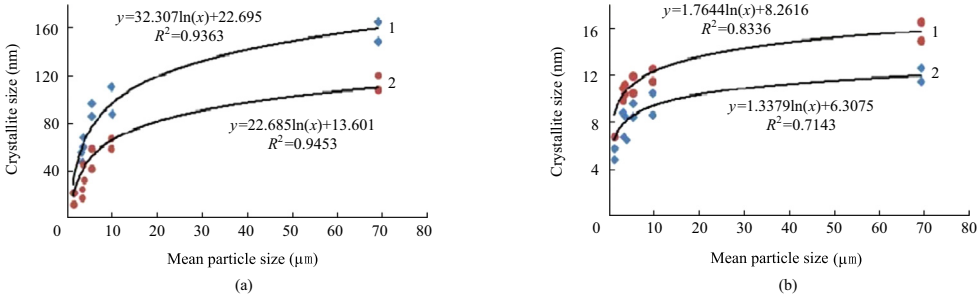

Fig. 6. Variation of the crystallite size of (a) quartz (1) and hematite (2) and (b) dolomite (1) and magnetite (2) powders as a function of mean particle size.

Table 4
Lattice parameters a, c and cell volume V of quartz, hematite, dolomite and magnetite samples extracted from the iron ore tailings.

Mineral	Parameters	Activation time (h)				
		0	1	2	6	12
Quartz	a (Å)	4.9101	4.915957	4.912479	4.914267	4.914076
	c (Å)	5.401273	5.408402	5.404535	5.406512	5.406331
	c/a	1.1000	1.1002	1.1002	1.1002	1.1002
	V (Å^3)	112.7736	113.192	112.9511	113.0747	113.0621
Hematite	a (Å)	5.030591	5.039091	5.033842	5.035615	5.033295
	c (Å)	13.74929	13.75363	13.74858	13.76059	13.77133
	c/a	2.7331	2.7294	2.7312	2.7327	2.7360
	V (Å^3)	301.3347	302.4492	301.7085	302.1848	302.1422
Dolomite	a (Å)	4.810735	4.815272	4.812266	4.803193	4.80102
	c (Å)	16.02736	16.04872	16.03102	16.08354	16.11671
	c/a	3.3316	3.3329	3.3313	3.3485	3.3569
	V (Å^3)	321.2295	322.2648	321.5074	321.3456	321.7170
Magnetite	a (Å)	8.391581	8.386535	8.379004		
	c (Å)	8.391581	8.386535	8.379004		
	c/a	1.0000	1.0000	1.0000		
	V (Å^3)	590.9237	589.8583	588.2707		

displays a significant variation in the lattice parameter c (0.089 Å after 12 h of milling, Fig. 7a), while the parameter a increases more drastically in quartz than in hematite and decreases monotonically in dolomite, showing a minor peak at the initial stage of milling (0.022 Å, Fig. 7b). The magnetite sample exhibits a reduction in the cell volume and «a» decrease of the lattice parameters after 6 h of activation.

The observed changes in structures of ferruginous quartzite tailings induced by extended milling provide additional information on the formation and growth of active absorption centers on the surface of waste tailings with a further decrease in particle size, which enhances the activity of particles with respect to cement and cement hydration products and improve the mechanical properties of composites manufactured using ferruginous quartzite backfills [27].

This allows a conclusion about mechanical activation of ferruginous quartzite tailings. It should be noted that mechanical activation and grinding cannot be considered as separate processes: any grinding process is activation since the action of the external forces leads to an increase in the energy of materials subjected to grinding [28]. The kinetic theory proposed by Boldyrev suggests that there are two main physical processes, which initiate chemical reactions in solids: crystal breakage and deformation. These processes lead to the development of point defects, linear defects (dislocations) and breakage of crystals accompanied by breakage of chemical bonds on the newly-formed surfaces and formation of higher activity centers. The main chemical reactions in this case are processes that take place at the contact points between particles and within fractures as well as at the high activity centers of the newly-formed surfaces [29].

The assumptions about the positive effects of mechanical activation of ferruginous quartzite tailings during milling as a result of changes in their structural and microstructural properties and surface activity centers on the strength of composite backfills were

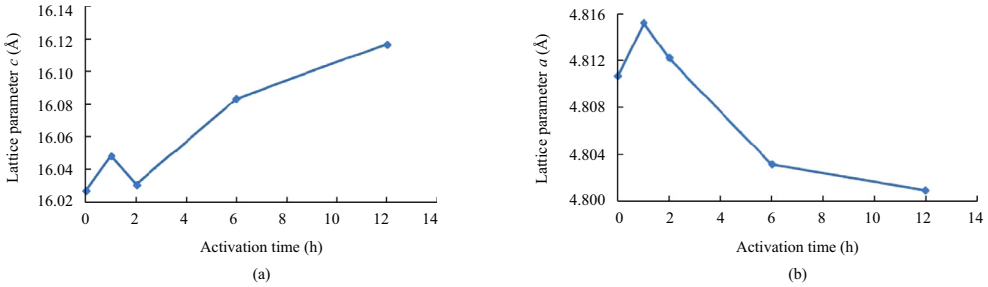

Fig. 7. Variation of the lattice parameter: (a) *c* and (b) *a* of dolomite as a function of the activation time.

supported by the results obtained on the samples subjected to the compressive stress for 180 of normal hardening. The addition of 2.67% (by weight) waste tailings milled to the 3.46 μm particle size to the backfill material, which also included Portland cement, sand and water, resulted in 12% increase in the compressive strength and 54.5% reduction in relative shrinkage. It should be noted that the ground waste tailings used in the experiment were stored for several months after mechanical activation. It is well known the activity of ground material is reduced during storage [30]. The most intense reduction is observed after the first 30 min of keeping in air, attaining the maximum value and stabilizing after 1–3 h of storage [31]. It can be expected that the use of fresh ground powders will increase the strength of composite backfills.

4. Conclusions

The experimental results presented in this study allow the following conclusions to be drawn:

(1) The results revealed that mechanical activation in the planetary mill causes substantial structural and morphological changes in the waste materials generated during beneficiation of ferruginous quartzite using the wet magnetic separation process as well as changes in the microstructural characteristics of the milled products.
(2) After 12 h of milling, the particle size of tailings was reduced from 69 to 1.22 μm. The variation in the crystallite size with milling time can be approximated by the exponential function at the 0.98 confidence level.
(3) Mechanical activation leads to changes in the particle shape. Elongation increases by 73% after 6 h of milling while after 12 h of milling the particles tend to be more rounded.
(4) The increase in the degree of crystallinity of hematite, magnetite, and dolomite can be explained by liberation of intergrowths and reaches its maximum in dolomite after 6 h of milling. The variations in the abundance of X-ray amorphous phase and the mean particle size of quartz powder, which can be approximated by a logarithmic function at the 0.987 confidence level, reaches 80% in powder samples with the mean particle size of 1.22 μm.
(5) The crystallite sizes obtained from the Williamson-Hall plots range from 149.7 to 20.1 nm for quartz, 108.6 to 21.1 nm for hematite, 11 to 4.8 nm for dolomite, 14.9 to 6.8 nm for magnetite, respectively, depending on the activation time. The variation in the crystallite size in the medium grain-sized powder samples can be well approximated by logarithmic functions. After 12 h of milling, the broadening of diffraction peaks is contributed both by the crystallite size and lattice strain.
(6) Mechanical activation leads to changes in the lattice parameters. It was found that the lattice parameters and unit cell volume exhibit different trends in different mineral powders during mechanical activation. This implies an expansion of the lattice parameters and unit cell volume for quartz, hematite, and dolomite and contraction for magnetite. The most significant change in the lattice parameter *c* (0.089 Å) was calculated for the dolomite sample.
(7) The mechanically induced structural changes in the waste generated from beneficiation of ferruginous quartzite during extended milling provide possibilities to use them as composite backfills to improve the mechanical and processing behavior of filling materials.

References

[1] Bhanwar SC, Santosh K. Underground void filling by cemented mill tailings. Int J Min Sci Technol 2013;23(6):893–900.
[2] Savitzky A, Golay MJE. Smoothing and differentiation of data by simplified least squares procedures. Anal Chem 1964;36(8):1627–39.
[3] Sonneveld EJ, Visser JW. Automatic collection of powder data fromphotographs. J Appl Cryst 1975;8(1):1–7.
[4] Racinger WA. A correction for the α_1:α_2 doublet in the measurement of widths of X-ray diffraction lines. J Sci Instrum 1948;25(7):254–9.
[5] Warren BE. X-ray diffraction. Dover: Dover Publications; 1990. p. 381.
[6] Williamson GK, Hall WH. X-ray line broadening from filed aluminium and wolfram. Act Metal 1953;1(1):22–31.
[7] Santra K, Chatterjee P, Sen Gupta SP. Voigt modeling of size-strain analysis: application to α-Al_2O_3 prepared by combustion technique. Bull Mater Sci 2002;25(3):251–7.
[8] Ermolovich EA, Izmest'ev KA, Kirilov AN. Fine-dispersed and nano mineral particles in mining and metallurgical wastes after commercial and laboratory grinding. J Min Sci 2012;48(1):188–94.
[9] Tkacova K. Mechanical activation of minerals. Amsterdam: Elsevier; 1989. p. 186.
[10] Pourghahramani P, Forssberg E. Comparative study of microstructural characteristics and stored energy of mechanically activated hematite in different grinding environments. Int J Miner Process 2006;79(2):120–39.
[11] Balaz P, Ficeriova J, Sepelak V, Kammel R. Thiourea leaching of silver from mechanically activated tetrahedrite. Hydrometallurgy 1996;43(1–3):367–77.
[12] Welham NJ, Llewellyn DJ. Mechanical enhancement of the dissolution of ilmenite. Miner Eng 1998;11(9):827–41.
[13] Welham NJ. Enhanced dissolution of tantalite, columbite following milling. Int J Miner Process 2001;61(3):145–54.
[14] Zhang Q, Kasai E, Saito F. Mechanochemical changes in gypsum when dry ground with hydrated minerals. Powder Technol 1996;87(1):67–71.
[15] Kaya E, Glogg R, Kumar SR. Particle shape modification in comminution. Kona Powder Particle J 2002;20(1):188–95.
[16] Kuga Y, Ma X, Koga J, Endoh S, Inoue I. Measurement and statistical analysis of shape of particles comminuted by a screen mill. Powder Technol 1985;44(3):281–90.
[17] Ohlberg SM, Strickler DW. Determination of percent crystallinity of partly devitrified glass by X-ray diffraction. J Am Ceram Soc 1962;45(4):170–1.
[18] Elmas E, Yildiz K, Toplan N, Toplan H Özkan. Effect of mechanical activation on mullite formation in an alumina-quartz ceramics system. Mater Technol 2013;47(4):413–6.
[19] Heegn H. Concerning some fundamentals of fine grinding. In: Procedings 1st world congress on particle technology, Part II. comminution, Nuremberg. p. 63–77.
[20] Mohammadnejad Sima, Provis John L, van Deventer Jannie SJ. Effects of grinding on the preg-robbing potential of quartz in an acidic chloride medium. Miner Eng 2013;52(10):31–7.
[21] Balaz P. Extractive metallurgy of activated minerals. Amsterdam: Elsevier; 2000. p. 299.
[22] Yusupov TS, Kirillova EA, Shumskaya LG. Mineral hardness effect on the combined mineral grinding. J Min Sci 2007;43(4):450–4.

[23] Arbain Roshaida, Othman Munirah, Palaniandy Samayamutthirian. Preparation of iron oxide nanoparticles by mechanical milling. Miner Eng 2011;24(1):1–9.
[24] Balaz P, Timko M, Kovac J, Bujnakova Z, Durisin J, Myndyk M, et al. Magnetic properties and sorption activity of mechanically activated magnetite Fe_3O_4. Acta Physica Polonica 2010;118(5):1005–7.
[25] Kaczmarek WA, Ninham BW. Preparation of Fe_3O_4 and γ-Fe_2O_3 powders by magnetomechanical activation of hematite. IEEE Trans Magn 1994;30 (2):732–4.
[26] Stewart SJ, Borzi RA, Cabanillas ED, Punte G, Mercader RC. Effects of milling-induced disorder on the lattice parameters and magnetic properties of hematite. J Magn Magn Mater 2003;260(3):447–54.
[27] Ermolovich EA. Effect of grinding on the donor–acceptor properties of surfaces of backfill mix components. J Min Sci 2013;49(5):839–46.
[28] Molchanov VI, Selezneva OG, Zhirnov EN. Activation of minerals during grinding. Moscow: Nedra; 1988.
[29] Boldyrev VV, Avvakumov EG, Boldyreva EV. Fundamental principles of mechanical activation, mechanosynthesis and mechanochemical technologies. Novosibirsk: SO RAN; 2009. p. 344.
[30] Komokhov PG, Shangina NN. Modified cement concrete, its structure and properties. Concr Appl 2002;1(1):43–6.
[31] Trautvain AI. Asphalt concrete manufactured with the use of mechanically activated silica-based mineral powders. Belgorod: BSTU After VG Shukhov; 2012. p. 24.